

NeuroPhysNet: A FitzHugh-Nagumo-Based Physics-Informed Neural Network Framework for Electroencephalograph (EEG) Analysis and Motor Imagery Classification

Zhenyu Xia¹[0009-0003-7374-7770], Xinlei Huang¹[0000-0002-4761-7652], and Suvash C. Saha¹[0000-0002-9962-8919]

University of Technology Sydney, Ultimo NSW 2007, Australia
suvash.saha@uts.edu.au

Abstract. Electroencephalography (EEG) is extensively employed in medical diagnostics and brain-computer interface (BCI) applications due to its non-invasive nature and high temporal resolution. However, EEG analysis faces significant challenges, including noise, nonstationarity, and inter-subject variability, which hinder its clinical utility. Traditional neural networks often lack integration with biophysical knowledge, limiting their interpretability, robustness, and potential for medical translation. To address these limitations, this study introduces NEUROPHYSNET, a novel Physics-Informed Neural Network (PINN) framework tailored for EEG signal analysis and motor imagery classification in medical contexts. NEUROPHYSNET incorporates the FitzHugh-Nagumo model, embedding neurodynamical principles to constrain predictions and enhance model robustness. Evaluated on the BCIC-IV-2a dataset, the framework achieved superior accuracy and generalization compared to conventional methods, especially in data-limited and cross-subject scenarios, which are common in clinical settings. By effectively integrating biophysical insights with data-driven techniques, NEUROPHYSNET not only advances BCI applications but also holds significant promise for enhancing the precision and reliability of clinical diagnostics, such as motor disorder assessments and neurorehabilitation planning.

Keywords: Physics-informed neural networks · EEG analysis · Motor imagery classification.

1 Introduction

Electroencephalography (EEG) is a widely used non-invasive technique for measuring the electrical activity of the brain, providing critical insights into various brain functions and disorders. Due to its high temporal resolution and ease of application, EEG has found widespread use in clinical and research settings, such as epilepsy diagnosis, sleep studies, and cognitive monitoring [27]. One particularly significant application of EEG is in Brain-Computer Interfaces (BCIs), where

EEG signals are used to establish direct communication pathways between the brain and external devices. Among BCI paradigms, motor imagery (MI) stands out as a prominent example. MI involves the mental rehearsal of movement without actual physical execution, and it plays a crucial role in developing assistive technologies for individuals with motor impairments [5].

Despite the potential of EEG in such applications, analyzing EEG signals remains challenging due to their inherent complexity. EEG signals are characterized by low spatial resolution, high noise levels, and nonstationarity, making it difficult to extract meaningful features [29]. Traditional neural networks, including multilayer perceptrons (MLPs) and convolutional neural networks (CNNs), have been extensively applied to process EEG signals. These models rely on learning complex patterns directly from data, often using handcrafted features or transformations such as spectral power analysis or spatial covariance matrices [22]. While these approaches have shown promise in certain scenarios, they suffer from several limitations. First, traditional methods typically lack the ability to incorporate prior biophysical knowledge about brain dynamics, limiting their interpretability and robustness across varying datasets [3]. Second, they are prone to overfitting in small datasets, which is a common scenario in medical applications [7]. Third, these models often struggle to generalize across subjects due to individual variability in brain dynamics [33].

Physics-Informed Neural Networks offer a promising alternative to address these limitations. The core advantage of PINNs lies in their ability to embed physical laws or domain-specific constraints directly into the learning process, thereby bridging the gap between data-driven methods and mechanistic understanding [8]. By explicitly incorporating physical rules or mathematical formulations within the model, PINNs seamlessly integrate traditional data modeling with physical modeling, enabling neural networks to not only learn complex patterns from data but also adhere to the underlying physical principles, enhancing the scientific validity of predictions.

In the context of EEG signal analysis, PINNs demonstrate unique advantages. The generation of EEG data is fundamentally governed by neurodynamical mechanisms, such as the variations in neuronal membrane potentials and the propagation of signals across nodes [32]. Traditional data-driven approaches often overlook these inherent physical constraints, while PINNs leverage neurodynamical models to capture these dynamics. These equations, known for their simplicity yet powerful functionality, describe the changes in neuronal membrane potential and recovery dynamics, providing a biophysically consistent representation of neural activity.

Moreover, the ability of PINNs to incorporate biophysical modeling enhances both the interpretability and generalizability of the model. Conventional machine learning methods commonly suffer from issues such as overfitting on small datasets and limited transferability across different datasets [6]. By embedding physical constraints, PINNs introduce a strong inductive bias, reducing dependency on large-scale labeled data and improving robustness against noise and shifts in data distribution [8]. Importantly, by linking the outputs of the neural

network directly to validated physical models, PINNs enable researchers to interpret the decision-making process of the model more effectively, a feature that is particularly crucial in medical applications where reliability is paramount.

Building on this foundation, this study introduces a novel PINN-based framework specifically designed for the analysis of EEG signals, with a particular focus on motor imagery classification. This framework integrates the FitzHugh-Nagumo model [11] into the learning process, leveraging its neurodynamical principles to constrain the predictions. By embedding this biophysical model, the framework ensures that the outputs adhere to well-established physiological laws, enhancing the reliability and interpretability of the results. In addition to incorporating the FitzHugh-Nagumo model, the framework includes a dedicated feature extraction module that processes the outputs of the PINN. This module extracts robust temporal features from the biophysically informed variables, such as membrane potentials and recovery dynamics, and transforms them into compact and discriminative representations suitable for downstream classification tasks. This step bridges the gap between physical modeling and modern classification techniques, ensuring that the extracted features retain both local temporal information and global biophysical relevance. By seamlessly combining biophysical modeling and data-driven neural network techniques, the proposed framework effectively addresses the limitations of traditional approaches. It mitigates the challenges of poor generalizability and limited interpretability, often observed in standard neural networks applied to EEG analysis. Furthermore, this integration allows the model to capture essential neurodynamical patterns while remaining flexible enough to adapt to the complex, nonlinear nature of EEG signals. As a result, the framework offers a more interpretable and generalizable solution for EEG-based applications

The primary contributions of this work are as follows:

- **Biophysical Modeling in EEG Analysis:** We introduce a PINN framework that integrates the FitzHugh-Nagumo model, enabling the incorporation of neurodynamical constraints into the analysis of EEG signals. This approach enhances the interpretability and robustness of the model.
- **Advanced Feature Extraction:** A novel feature extraction module is designed to process the biophysically informed outputs of the PINN. This module extracts temporal features at the node level while preserving the physical consistency of the data, resulting in compact and discriminative representations.
- **Application to Motor Imagery Classification:** We demonstrate the effectiveness of the proposed framework in motor imagery classification tasks, achieving improved performance and generalization compared to traditional neural network approaches. The results underscore the potential of combining biophysical modeling with modern neural network architectures in medical applications.

2 Related Work

2.1 Deep Learning in BCI-MI Analysis

Recent advances in deep learning have substantially enhanced the performance of BCIs for MI analysis, particularly through the use of CNNs and Recurrent Neural Networks (RNNs). These techniques have demonstrated notable improvements in classification accuracy for MI tasks, as shown in several key studies.

Schirrmeister et al. demonstrated the potential of CNNs in EEG decoding and visualization, showcasing the ability of deep learning models to extract meaningful features from EEG signals for improved classification [25]. Similarly, Lawhern et al. introduced EEGNet, a compact CNN architecture specifically designed for efficient EEG-based BCI applications, further advancing the state of the art in MI classification [17]. Huang et al. also investigated CNN-based deep learning models for MI classification, highlighting their superior performance in classification accuracy compared to traditional methods [9]. The low SNR in MI EEG signals poses a challenge in decoding movement intentions, but this can be addressed using multi-branch CNN modules that learn spectral-temporal domain features, as suggested in [13]. Furthermore, Ju et al. proposed Tensor-CSPNet [16] and Graph-CSPNet [14], a novel geometric deep learning framework for motor imagery classification, achieving improved feature extraction, robustness, and interpretability.

Despite their success, deep learning approaches for MI analysis face several inherent limitations. First, they are heavily data-dependent, requiring large labeled datasets for training, which is often not feasible in medical applications with limited data. This leads to issues of overfitting, particularly when working with small datasets. Furthermore, deep learning models are often criticized for their "black box" nature, which hinders their interpretability and transparency—crucial factors for medical applications. Additionally, due to inter-subject variability and differences in brain dynamics, deep learning models often struggle with generalization, limiting their ability to perform reliably across diverse datasets. Lastly, complex neural network architectures tend to result in long training and inference times, making them less suitable for real-time applications in BCIs.

2.2 Physics-Informed Neural Networks in BCI-MI Analysis

To address the aforementioned limitations of traditional deep learning models, PINNs have emerged as a promising alternative. PINNs combine data-driven deep learning methods with physical constraints derived from underlying scientific principles, offering enhanced interpretability, generalization, and robustness.

Raissi et al. first introduced the concept of PINNs as a method for solving forward and inverse problems involving nonlinear partial differential equations (PDEs). Their work demonstrated how incorporating physical laws directly into the learning framework can improve the accuracy and generalization of deep learning models. This approach has since been extended to various domains, including the study of dynamic systems in neurodynamics and brain modeling,

which are directly relevant to EEG signal analysis in BCI applications. In particular, PINNs offer a powerful tool for modeling the brain's biophysical dynamics during motor imagery tasks [1].

Lu et al. explored the use of Physics-Informed DeepONets, an extension of PINNs, for solving parametric PDEs. Their work highlights the ability of PINNs to generalize across different parametric settings, a feature that could be applied to EEG signal analysis, where individual differences in brain activity need to be accounted for. The inclusion of such models could improve the performance of BCIs by better capturing the underlying neurodynamical processes during MI tasks [31]. Zhang et al. proposed a framework to quantify uncertainty in PINNs, which is particularly beneficial for handling noisy EEG data and improving the robustness of models, as uncertainty quantification is crucial in BCI applications where data quality is often variable [34].

Further advancements have been made in improving the convergence and efficiency of PINNs. Jagtap et al. introduced adaptive activation functions that accelerate the training process, reducing the computational burden and improving the model's performance. This innovation is particularly relevant in the context of real-time BCI applications, where fast and accurate predictions are necessary for immediate feedback to users [12]. Chen et al. applied PINNs to heat transfer problems, demonstrating the potential of such methods in improving model accuracy by incorporating physical constraints. Although their focus was not on EEG signals, the general principle of embedding physical models into the neural network has significant implications for brain signal processing [4].

In the context of long-term integration of parametric ordinary differential equations (ODEs), Wang et al. explored how PINNs could be applied to such problems, providing insights into modeling dynamic systems over extended periods. This capability is essential for BCI-MI systems, where the brain's activity during motor imagery may evolve over time and require long-term temporal modeling [30]. The application of PINNs in fluid dynamics, as demonstrated by Mao, showcases how complex physical phenomena can be captured through neural networks. This approach can be extended to model the complex dynamics of brain activity, where non-linear interactions between different brain regions play a key role in motor imagery tasks [24].

Our proposed method, which integrates the FitzHugh-Nagumo model within a PINN framework, addresses several of the limitations associated with both deep learning and traditional PINN approaches. By embedding biophysical knowledge directly into the learning process, our model offers enhanced interpretability, a crucial factor for medical applications. The incorporation of physical constraints also reduces the model's dependence on large labeled datasets, improving generalization across individuals and datasets. Furthermore, the robustness of the approach is enhanced, as the physical constraints allow the model to better handle noise and individual variations in EEG signals. The integration of data-driven techniques with biophysical models in our framework ensures that the model's predictions are aligned with established physiological laws, providing a more scientifically grounded approach to EEG signal analysis in BCI applications.

3 Methodology

In this study, we develop a PINN based on the FitzHugh-Nagumo (FHN) model to analyze and interpret EEG data for BCI applications. The proposed architecture seamlessly integrates domain-specific physiological laws with advanced deep learning techniques, thereby enhancing predictive performance and ensuring adherence to biophysical consistency. This section outlines the mathematical foundations, architectural design, and implementation details of the FHN-informed PINN framework.

3.1 FitzHugh-Nagumo Model

The FHN model stands as a seminal framework in the study of neuronal dynamics, offering a simplified yet robust representation of the essential electrical activities within neurons. Introduced by Richard FitzHugh and Julius Nagumo in the 1960s, the FHN model was conceived to streamline the more intricate Hodgkin-Huxley model while retaining the fundamental characteristics of neuronal action potentials. The Hodgkin-Huxley model details the ionic mechanisms underlying action potentials, providing a precise description of neuronal electrical activity. However, its high dimensionality and complexity pose significant challenges for large-scale network simulations and theoretical analyses. In contrast, the FHN model reduces the number of variables and parameters, presenting a more tractable form to describe the excitation and recovery processes of neurons, thereby facilitating more efficient and feasible analyses and simulations of neural dynamics.

Mathematically, the FHN model is articulated through a pair of coupled nonlinear ordinary differential equations that describe the temporal evolution of two critical variables: the activation variable u and the recovery variable v . These equations are given by:

$$\begin{cases} \frac{du}{dt} = u - \frac{u^3}{3} - v + I \\ \frac{dv}{dt} = \epsilon(u + a - bv) \end{cases} \quad (1)$$

where u typically represents the membrane potential or the excitatory state of the neuron, while v corresponds to the recovery processes, such as the activation of potassium ion channels that restore the neuron to its resting state after an action potential. I denotes the external stimulus current applied to the neuron, driving its activity. The parameter ϵ is a small positive constant that signifies the separation of timescales between the fast dynamics of the activation variable and the slower dynamics of the recovery variable. The constants a and b are system parameters that govern the behavior and dynamical characteristics of the model. t represents the time variable, describing the evolution of the system over time, and these differential equations reflect the dynamics of the membrane potential u and the recovery variable v as functions of t .

Despite its reduced complexity, the FHN model adeptly captures the cyclical nature of neuronal firing, encompassing the transition from a quiescent state

to an excited state and back to rest. This cyclical behavior is emblematic of the generation and propagation of action potentials in real neurons. The FHN model exhibits a rich array of dynamical phenomena, including limit cycle oscillations, bifurcations, and chaotic dynamics, contingent upon the values of the parameters ϵ , a , and b . Under varying parameter regimes, the model can display distinct behaviors such as stable fixed points (resting states), periodic oscillations (reflecting repetitive firing of action potentials), and chaotic dynamics (indicating complex, aperiodic neuronal activity). These characteristics render the FHN model not only a valuable theoretical tool for understanding neuronal behavior but also a practical model for simulating and analyzing complex neural systems.

In the context of EEG modeling, the FHN model offers several compelling advantages that align with the intricate dynamics observed in brain activity. EEG is a non-invasive technique that records electrical activity generated by large populations of neurons, providing rich spatiotemporal information about brain function. The signals captured by EEG reflect the synchronous firing and oscillatory behavior of neuronal assemblies across different brain regions, encompassing a wide range of frequency bands associated with various cognitive and physiological states.

One of the primary motivations for employing the FHN model in EEG modeling is its ability to encapsulate the core dynamical features of neuronal activity with a minimal set of variables and parameters. The simplicity of the FHN model facilitates the analysis and simulation of large-scale neural networks, which is essential for interpreting EEG data that arise from the collective behavior of thousands to millions of neurons. By reducing the dimensionality of the problem, the FHN model allows for more tractable mathematical and computational treatments, enabling researchers to focus on the essential dynamics without being overwhelmed by the complexity of the underlying biological processes.

Moreover, the FHN model's capacity to represent both excitatory and inhibitory interactions makes it particularly suited for capturing the balance of neural excitation and inhibition that is crucial for normal brain function. This balance is reflected in EEG signals, where different oscillatory patterns emerge from the interplay between excitatory and inhibitory neural populations. The nonlinear dynamics of the FHN model are adept at reproducing these oscillatory patterns, providing a mechanistic basis for understanding the generation of EEG rhythms such as alpha, beta, and gamma waves.

Another significant advantage of the FHN model in EEG modeling lies in its flexibility and scalability. The model can be easily extended to incorporate additional complexities, such as spatial interactions between neurons or the inclusion of external inputs that mimic sensory stimuli or cognitive tasks. This adaptability is particularly beneficial for applications in BCI, where EEG signals are utilized to decode and interpret specific mental states or intentions, such as motor imagery. The FHN model can be integrated into advanced computational frameworks, such as PINNs, to enhance the accuracy and robustness of EEG signal interpretation by embedding biophysical constraints directly into the learning process.

Furthermore, the FHN model serves as a bridge between theoretical neuroscience and practical applications in medical technology. By providing a clear and interpretable model of neuronal dynamics, the FHN framework facilitates the development of algorithms capable of accurately decoding EEG signals in real-time applications. This is particularly relevant for BCI systems aimed at assisting individuals with motor impairments, where precise and reliable interpretation of EEG data is paramount for effective control of prosthetic devices or communication aids.

In addition to its theoretical and practical utility, the FHN model's ability to generate simulation data that can be compared with experimental EEG recordings offers a robust mechanism for validating and refining signal processing algorithms. By simulating EEG signals under various conditions and tasks, researchers can systematically evaluate the performance of different modeling approaches and optimize parameters to achieve better alignment with empirical data. This iterative process enhances the reliability and validity of EEG-based models, ensuring that they accurately reflect the underlying neural dynamics.

In conclusion, the FHN model, with its balanced combination of simplicity and dynamical richness, emerges as an indispensable tool for EEG modeling in the realm of BCI applications. Its ability to capture the fundamental aspects of neuronal excitability and inhibition, coupled with its computational efficiency and scalability, provides a solid foundation for developing sophisticated models that can interpret complex brain signals with high accuracy. The integration of the FHN model into frameworks like PINNs not only enhances predictive performance but also ensures the physical consistency of model outputs, thereby bridging the gap between theoretical neuroscience and practical medical applications. As such, the FHN model significantly contributes to advancing our understanding of neural dynamics and driving the development of effective BCI technologies for medical rehabilitation and human-machine interfacing.

3.2 Design and Implementation of a Physics-Informed Neural Network Based on the FitzHugh-Nagumo Model

In this study, we present the design and implementation of a PINN architecture grounded in the FHN model for the analysis and interpretation of EEG data. The proposed PINN architecture is structured into three components: the “Data Preprocessing Module”, the “Feature Extraction Module”, and the “PINN Model”. This hierarchical design facilitates the transformation of raw EEG signals into a structured format, the extraction of pertinent features, the incorporation of biophysical constraints through the FHN model, and the subsequent classification of specific tasks such as motor imagery. The integration of these modules ensures enhanced predictive performance, robustness, and adherence to the underlying physical principles governing neuronal dynamics.

Data Preprocessing Module The Data Preprocessing Module serves as the initial stage of the PINN architecture, responsible for converting raw EEG time-

series data into a structured format that is conducive to subsequent processing and analysis. Specifically, the input EEG data is reorganized into a four-dimensional tensor with the shape $W \times F \times C \times \omega$, where W represents the number of window slices, F denotes the number of filter banks, C corresponds to the number of EEG channels, and ω signifies the window length.

This transformation is critical for effectively capturing the spatiotemporal dynamics inherent in EEG signals. The process involves three key steps: temporal segmentation and frequency decomposition.

Temporal segmentation involves dividing the continuous EEG signal into smaller, manageable segments known as window slices. Given an input EEG tensor $\mathbf{X} \in \mathbb{R}^{B \times C \times T}$, where B denotes the batch size, C is the number of EEG channels, and T represents the total number of time points, the temporal segmentation can be expressed as:

$$\mathbf{X}' = \text{Temporal_Segmentation}(\mathbf{X}) \in \mathbb{R}^{B \times W \times C \times \omega}, \quad (2)$$

where W represents the number of window slices, C corresponds to the number of EEG channels, and ω signifies the window length. The segmentation aims to divide EEG signals into small segments on the time domain, either with overlapping or without overlapping. This division facilitates the detailed analysis of temporal dynamics within each window, allowing the model to capture transient features that may be indicative of specific cognitive or motor states.

Frequency decomposition is achieved through the application of filter banks, which decompose each windowed EEG signal into multiple frequency passbands. Mathematically, this can be represented as:

$$\mathbf{X}'' = \text{FilterBank_Decomposition}(\mathbf{X}') \in \mathbb{R}^{B \times W \times F \times C \times \omega}, \quad (3)$$

where F denotes the number of filter banks applied. Utilizing causal Chebyshev Type II filters, the raw oscillatory EEG signals are decomposed into distinct frequency bands. This decomposition is essential for isolating frequency-specific information corresponding to various neural oscillations, such as alpha, beta, and gamma waves, each associated with different cognitive and physiological functions. By separating the EEG signals into these frequency bands, the model can more effectively capture the nuanced patterns and interactions that occur within specific frequency ranges.

3.3 Physics-Informed Neural Network Module

The PINN module is the central component of the proposed architecture, responsible for integrating the FHN model's biophysical constraints with the structured EEG data. This integration ensures the model's predictions adhere to the underlying physical principles of neuronal dynamics, providing accurate and interpretable results.

Input Processing and Convolutional Layers The model accepts input \mathbf{X}'' in the shape $B \times W \times F \times C \times \omega$. To align the input data with the convolutional layers, the tensor is reshaped into $(B \times W) \times F \times C \times \omega$, effectively merging the batch and window dimensions. This reshaped tensor is passed through two 2D convolutional layers, each followed by batch normalization and ReLU activation to stabilize the learning process and introduce non-linearity. These layers capture spatiotemporal patterns in the EEG data, which are crucial for modeling neuronal dynamics. The operations are mathematically represented as:

$$\mathbf{X}_1 = \text{ReLU}(\text{BatchNorm}(\text{Conv2D}(\mathbf{X}'', F_1, k_1, p_1))) \quad (4)$$

$$\mathbf{X}_1^{\text{pool}} = \text{MaxPool2D}(\mathbf{X}_1, p, s) \quad (5)$$

$$\mathbf{X}_2 = \text{ReLU}(\text{BatchNorm}(\text{Conv2D}(\mathbf{X}_1^{\text{pool}}, F_2, k_2, p_2))) \quad (6)$$

$$\mathbf{X}_2^{\text{pool}} = \text{MaxPool2D}(\mathbf{X}_2, p, s) \quad (7)$$

where F_1 and F_2 are the numbers of filters, k_1 and k_2 are kernel sizes, and p_1 , p_2 are paddings. Pooling layers downsample the feature maps, reducing temporal and spatial dimensions while retaining the most salient features. Here, p represents the pooling kernel size, determining the dimensions of the pooling operation, and s represents the stride, which defines the step size for the pooling filter as it slides over the feature map.

Fully Connected Layer The flattened output of the convolutional layers is processed by a fully connected layer, which projects the high-dimensional convolutional features into a lower-dimensional hidden representation. Dropout regularization is applied after the fully connected layer to prevent overfitting:

$$\mathbf{h}' = \text{Dropout}(\text{ReLU}(\mathbf{W}_{\text{fc}} \cdot \text{Flatten}(\mathbf{X}_2^{\text{pool}}) + \mathbf{b}_{\text{fc}})), \quad (8)$$

where \mathbf{W}_{fc} and \mathbf{b}_{fc} represent the weights and biases of the fully connected layer, respectively.

Transformer Encoder for Temporal Dependencies The hidden representation is passed through a Transformer encoder to model long-range dependencies in the temporal dimension. The Transformer encoder, consisting of multiple layers of multi-head self-attention and feed-forward networks, captures the temporal relationships necessary for decoding EEG signals:

$$\mathbf{H} = \text{TransformerEncoder}(\mathbf{h}') \quad (9)$$

The encoder processes the input sequence of embeddings and outputs contextualized representations:

$$\mathbf{H} \in \mathbb{R}^{(B \times W) \times \text{hidden_dim}} \quad (10)$$

Output Layer and Reshaping The Transformer output is fed into a linear layer that maps the hidden representation to the activation (v) and recovery (w) variables for each neuronal node across time. These variables are fundamental to the FHN model:

$$\mathbf{O} = \mathbf{W}_{\text{out}} \cdot \mathbf{H} + \mathbf{b}_{\text{out}} \quad (11)$$

The output tensor \mathbf{O} is reshaped to [batch_size, sliding_windows, $2 \times \text{num_nodes}$, data_points], where num_nodes represents the number of nodes in the graph, and data_points denotes the feature dimensions for each node. The first num_nodes along the node dimension is extracted as v , while the remaining num_nodes is extracted as w :

$$\mathbf{v} = \mathbf{O}[:, :, : \text{num_nodes}, :] \quad \mathbf{w} = \mathbf{O}[:, :, \text{num_nodes} :, :] \quad (12)$$

Design Rationale Compared to traditional PINNs, which primarily rely on MLPs, the PINN model proposed in this study incorporates a combination of CNNs and Transformer encoders. This design not only offers significant advantages in processing complex EEG data but also demonstrates superior capabilities in solving the key variables v and w of the FHN model.

Traditional PINNs with MLP-based architectures often struggle to effectively capture local spatiotemporal features and long-range dependencies in high-dimensional time-series data. MLPs process input data through fully connected layers without leveraging the spatial and temporal structures of the data. This lack of structural awareness can lead to inefficient feature extraction and reduced accuracy, particularly in estimating the activation variable v and recovery variable w .

In this study, CNNs are introduced as the feature extraction module to capture local spatiotemporal features from EEG signals. By using the convolutional kernels, CNN layers scan input signals along the temporal dimension to identify localized patterns and variations. These localized features are critical for accurately modeling the dynamics of v and w in the FHN model. Moreover, the application of Batch Normalization and ReLU activation functions enhances the stability of model training and improves the representation of non-linear features, further benefiting the calculation of v and w .

Additionally, Transformer encoders are integrated into the PINN model to capture long-range temporal dependencies. EEG signals often exhibit correlations over extended time spans, which are challenging for traditional convolutional operations to capture effectively. Transformers utilize multi-head self-attention mechanisms to dynamically evaluate relationships across different time points, enabling the model to construct global dependencies. This mechanism provides richer temporal context, ensuring that v and w are calculated with higher physical consistency and dynamic precision.

By combining CNNs and Transformers, the proposed model achieves efficient extraction of both local and global features while ensuring the accurate computation of v and w under the constraints of the FHN equations. This design significantly outperforms traditional MLP-based PINNs by producing results

that are more robust and precise when applied to complex EEG data. Furthermore, the inclusion of biophysical constraints ensures that the predicted v and w are not only accurate but also aligned with the underlying biological dynamics, enhancing the interpretability and reliability of the predictions.

physics-based Loss Function Given the predicted values v and w , the time derivatives are approximated using the finite difference method:

$$\frac{dv}{dt} \approx \frac{v(t + \Delta t) - v(t)}{\Delta t} \quad (13)$$

$$\frac{dw}{dt} \approx \frac{w(t + \Delta t) - w(t)}{\Delta t} \quad (14)$$

where Δt is the time step.

The residuals for v and w are computed as:

$$f_v = \frac{dv}{dt} - \left(v - \frac{v^3}{3} - w + I \right) \quad (15)$$

$$f_w = \frac{dw}{dt} - \epsilon(v + a - bw) \quad (16)$$

The physics-based loss is then defined as the mean squared error (MSE) of these residuals:

$$\mathcal{L}_{\text{physics}} = \frac{1}{N} \sum_{i=1}^N (f_{v,i}^2 + f_{w,i}^2) \quad (17)$$

where N is the total number of data points.

Coupling Term To model the interactions among nodes, a coupling matrix K is introduced. The modified dynamics for v incorporating coupling are given by:

$$\frac{dv}{dt} = v - \frac{v^3}{3} - w + I + \sum_j K_{ij}(v_j - v_i), \quad (18)$$

where K_{ij} represents Coupling strength between node i and node j , v_j is Membrane potential of node j , and v_i is Membrane potential of node i .

The coupling matrix K is defined as:

$$K_{ij} = \begin{cases} \text{coupling_strength,} & \text{if } i \neq j \\ 0, & \text{if } i = j \end{cases} \quad (19)$$

where coupling strength is set to 0.1, and the coupling matrix K , with a shape of [num_nodes, num_nodes], is initialized as an all-ones matrix with its diagonal elements subtracted by 1 and then multiplied by the coupling strength. The number of nodes.

The residual for v including coupling is given by:

$$f_v = \frac{dv}{dt} - \left(v - \frac{v^3}{3} - w + I + \sum_j K_{ij}(v_j - v_i) \right) \quad (20)$$

Final Physics Loss

$$\mathcal{L}_{\text{physics}} = \frac{1}{N} \sum_{i=1}^N \left[\left(\frac{d\hat{v}_i}{dt} - \hat{v}_i + \frac{\hat{v}_i^3}{3} + \hat{w}_i - I \right)^2 + \left(\frac{d\hat{w}_i}{dt} - \epsilon(\hat{v}_i + a - b\hat{w}_i) \right)^2 \right], \quad (21)$$

where \hat{v}_i and \hat{w}_i are the predicted membrane potential and recovery variables, respectively. I denotes the external stimulus, and ϵ , a , and b are parameters of the FHN model. For this study, these parameters are set as follows: $\epsilon = 0.08$, $a = 0.7$, $b = 0.8$, and $I = 0.5$.

This physics-based constraint ensures that the predictions follow the temporal dynamics governed by the FHN equations, enhancing the interpretability and reliability of the model.

Advantages This formulation of the physics-based loss:

- Ensures that the predictions v and w adhere to the FHN model's dynamics, maintaining physical consistency.
- Accounts for interactions among nodes through the coupling term, enabling a realistic representation of network dynamics.
- Uses finite differences to compute time derivatives, reducing computational complexity compared to backpropagation through time.

3.4 Feature Extraction Module

The Feature Extraction Module processes the outputs of the PINN model, specifically the FHN variables v (membrane potentials) and w (recovery variables). Each variable is processed independently to extract node-specific temporal features, and these features are later fused for downstream tasks. The module is invoked twice: once for v and once for w , ensuring that the extracted features capture distinct yet complementary temporal patterns inherent to these biophysically informed variables.

The inputs to the module are tensors $\mathbf{v} \in \mathbb{R}^{B \times N \times T}$ and $\mathbf{w} \in \mathbb{R}^{B \times N \times T}$, where B represents the batch size, N is the number of nodes (e.g., EEG channels), and T is the number of time points. To align the input tensors with the convolutional layers, the module reshapes and permutes the data into $\mathbf{v}_{\text{input}}, \mathbf{w}_{\text{input}} \in \mathbb{R}^{(B \cdot N) \times 1 \times T}$. This restructuring ensures that each node is treated as an independent input sequence while sharing the same weights across all nodes.

The module applies a sequence of one-dimensional convolutional layers to capture localized temporal dependencies. For the input $\mathbf{v}_{\text{input}}$, the operation of the first convolutional layer is given by:

$$\mathbf{v}_1 = \text{ReLU}(\text{BatchNorm}(\text{Conv1D}(\mathbf{v}_{\text{input}}, F_1, k, p))), \quad (22)$$

where F_1 represents the number of filters, k is the kernel size, and p is the padding. To further reduce the temporal resolution, a max-pooling operation is performed:

$$\mathbf{v}_1^{\text{pool}} = \text{MaxPool1D}(\mathbf{v}_1, k_p, s_p), \quad (23)$$

where k_p and s_p denote the pooling kernel size and stride.

The pooled features are passed through a second convolutional layer with an increased number of filters, refining the temporal features:

$$\mathbf{v}_2 = \text{ReLU} \left(\text{BatchNorm} \left(\text{Conv1D}(\mathbf{v}_1^{\text{pool}}, F_2, k, p) \right) \right), \quad (24)$$

followed by another max-pooling operation:

$$\mathbf{v}_2^{\text{pool}} = \text{MaxPool1D}(\mathbf{v}_2, k_p, s_p). \quad (25)$$

After the final pooling operation, the feature maps are flattened into one-dimensional vectors:

$$\mathbf{v}_{\text{flat}} = \text{Flatten}(\mathbf{v}_2^{\text{pool}}), \quad (26)$$

and then processed through a fully connected layer to map the extracted temporal features into a latent space:

$$\mathbf{v}_{\text{fc}} = \text{ReLU} (\mathbf{W}_{\text{fc}} \cdot \mathbf{v}_{\text{flat}} + \mathbf{b}_{\text{fc}}). \quad (27)$$

The same operations are applied independently to \mathbf{w} , producing:

$$\mathbf{w}_{\text{fc}} = \text{ReLU} (\mathbf{W}_{\text{fc}} \cdot \text{Flatten}(\mathbf{w}_2^{\text{pool}}) + \mathbf{b}_{\text{fc}}). \quad (28)$$

Finally, the outputs of v and w are fused through element-wise addition:

$$\mathbf{f} = \text{LayerNorm}(\mathbf{v}_{\text{fc}} + \mathbf{w}_{\text{fc}}), \quad (29)$$

where $\mathbf{f} \in \mathbb{R}^{B \times N}$ represents the fused feature matrix, which is passed to the next stage of the pipeline.

This design ensures that the module efficiently extracts complementary features from v and w while maintaining computational efficiency and scalability. By extracting temporal features from the biophysical variables v and w output by the PINN, the module not only captures local temporal dependencies but also integrates information constrained by physical laws, transforming it into enhanced network representations. These physically informed features serve a dual purpose within the network: on the one hand, they act as an augmentation mechanism, enhancing the network's representation capability for input data, thus improving the robustness and discriminative power of features beyond physical constraints; on the other hand, the inclusion of physical information provides a solid foundation for interpretability, ensuring that the final output aligns with the fundamental principles of neuronal dynamics at the feature level.

This feature enhancement strategy is particularly well-suited for handling the complex nature of EEG data. EEG signals exhibit strong spatiotemporal correlations and nonlinear characteristics, and the variables v and w generated by the

PINN not only result from data-driven processes but also incorporate physical constraints from the FHN model. These physical insights are transformed by the feature extraction module into high-dimensional representations that are more meaningful for downstream classification or regression tasks. This approach effectively addresses the lack of physical consistency often observed in traditional neural networks, such as MLPs or standard convolutional networks, when processing EEG data, while also mitigating performance fluctuations caused by distributional biases in the data.

Moreover, embedding physical information in the feature extraction process enhances the model’s generalization capability and provides critical support for cross-domain applications, such as BCI and medical diagnostics. By deeply leveraging the features of v and w , this design enables the network to better capture key patterns hidden within signals, significantly improving the overall performance on specific tasks, such as motor imagery classification or brain activity recognition. This method also demonstrates the potential of combining physical modeling with data-driven approaches, paving the way for future advancements in intelligent signal processing and neuronal dynamics modeling.

4 Experimental Design

4.1 Loss Function and Training

The training process was conducted over 100 epochs on a desktop computer equipped with an NVIDIA GeForce RTX 4090 GPU. The proposed NEUROPHYSNET framework optimizes a composite loss function that integrates both classification and physics-based objectives, aligning model predictions with both the observed EEG data and the underlying neurodynamic principles. The total loss is defined as:

$$\mathcal{L} = \mathcal{L}_{\text{classification}} + \lambda \mathcal{L}_{\text{physics}}, \quad (30)$$

where $\mathcal{L}_{\text{classification}}$ is the cross-entropy loss, which ensures accurate classification of MI tasks. Meanwhile, $\mathcal{L}_{\text{physics}}$ enforces the biophysical consistency of the predictions by adhering to the FHN model (see Eq. 21).

During training, a batch size of 64 and an initial learning rate of $1e^{-3}$ were used to ensure stable convergence. The weight parameter λ controls the trade-off between the classification and physics-based loss components, allowing the model to balance predictive accuracy with adherence to biophysical principles.

For inference, the framework was deployed on a desktop computer equipped with an NVIDIA GeForce RTX 2080Ti GPU. This setup efficiently processed EEG data for MI classification tasks, leveraging the neurodynamic insights embedded in the PINN architecture. By combining data-driven classification objectives with physics-based modeling, NEUROPHYSNET achieves robust and interpretable performance, addressing the challenges of generalization and reliability in medical EEG applications.

4.2 Dataset and Baseline Models

Dataset The BCIC-IV-2a dataset [26] is a widely used benchmark in EEG-based MI classification research, particularly in the context of BCI development. This dataset contains EEG recordings from nine subjects performing a four-class motor imagery task. The four classes include imagined movements of the left hand, right hand, both feet, and tongue. These tasks were chosen to activate distinct cortical areas, facilitating the analysis and classification of MI-related EEG signals.

Data Collection and Setup The EEG signals were recorded using 22 EEG electrodes placed according to the international 10-20 system, along with three electrooculography (EOG) channels to monitor eye movements. The signals were sampled at 250 Hz, providing high temporal resolution suitable for analyzing cortical dynamics during motor imagery. Each subject participated in two sessions: a training session and an evaluation session. Each session comprised six runs, with 12 trials per class, resulting in a total of 288 trials per subject.

Preprocessing For the experiments in this study, the EEG signals were preprocessed to enhance the signal-to-noise ratio and extract relevant features. The preprocessing pipeline included band-pass filtering to isolate task-relevant frequency bands (e.g., mu and beta rhythms), artifact removal using EOG channels, and segmentation into fixed-length temporal windows aligned with the onset of motor imagery tasks. These steps ensured that the dataset was ready for input into the proposed NEUROPHYSNET framework.

Significance in This Study The BCIC-IV-2a dataset serves as a robust benchmark to evaluate the proposed NEUROPHYSNET framework. Its well-annotated structure and realistic challenges, such as inter-subject variability and noise, provide a comprehensive testbed for assessing the generalization and interpretability of the physics-informed neural network architecture. By leveraging this dataset, we demonstrate the ability of NEUROPHYSNET to effectively integrate biophysical constraints and extract discriminative features for motor imagery classification.

Baseline Models To evaluate the performance and generalization capability of NEUROPHYSNET, we compared it against a comprehensive set of baseline methods, categorized as follows:

– **CSP-Based Methods:**

- Filter Bank Common Spatial Pattern (FBCSP) [2]: A classical approach that applies spatial filters across multiple frequency bands to extract task-relevant features from EEG signals.

– **Riemannian Geometry-Based Methods:**

- Minimum Distance to Mean (MDM) [28]: Classifies EEG signals by minimizing geodesic distances between covariance matrices.

- Temporal Spectral Mapping (TSM) [19]: Combines temporal and spectral features to improve classification performance.
- SPDNet [10]: A deep learning model specifically designed to process symmetric positive definite (SPD) matrices.
- Tensor-CSPNet [15]: Extends CSP by incorporating tensor-based feature representations.
- **Deep Learning Architectures:**
 - ConvNet [20]: A simple convolutional neural network optimized for EEG feature extraction.
 - EEGNet [18]: A compact and efficient architecture designed specifically for brain-computer interface (BCI) applications.
 - Filter Bank Convolutional Network (FBCNet) [23]: Integrates filter banks with convolutional networks to extract multi-band EEG features.

These baselines represent a diverse array of strategies, allowing us to evaluate NEUROPHYSNET’s performance in comparison to traditional CSP methods, advanced Riemannian geometry-based approaches, and cutting-edge deep learning models.

Fusion of v and w with Tensor-CSPNet Features The fusion process combines v and w features with the high-dimensional tensor features produced by Tensor-CSPNet’s layers. This integration occurs at the feature level, where the outputs of Tensor-CSPNet’s feature extraction module are concatenated with the physiological The fusion process combines v and w features with the high-dimensional tensor features produced by Tensor-CSPNet’s layers. Tensor-CSPNet, as a state-of-the-art technique, has demonstrated outstanding performance in EEG classification tasks due to its ability to capture complex spatial and frequency characteristics of EEG signals. By leveraging advanced tensor representations, Tensor-CSPNet provides a strong foundation for feature extraction, making it one of the most effective models in this domain.

This integration occurs at the feature level, where the outputs of Tensor-CSPNet’s feature extraction module are concatenated with the physiological features. The fused feature set is then passed through additional neural layers for final classification. This approach allows the model to simultaneously leverage spatial, frequency, temporal, and physiological dynamics, enhancing its ability to discriminate between EEG classes.

5 Experimental Results

5.1 NEUROPHYSNET Generalization Performance vs. Leading-Edge Methodologies

To evaluate the performance and generalization capability of NeuroPhysNet, we compared it against a range of baseline models across cross-validation (CV) and Holdout scenarios on the BCIC-IV-2a dataset. Table 1 summarizes the results,

Table 1: Comparative Analysis of Subject-Specific Accuracies and Standard Deviations in BCIC-IV-2a Dataset.

	CV (T)	Acc %	CV (E)	Acc %	Holdout (T → E)	Acc %
FBCSP [2]	71.29		73.39		66.13	
EEGNet [18]	69.26		66.93		60.31	
ConvNet [20]	70.42		65.89		57.61	
FBCNet [23]	75.48		77.16		71.53	
MDM [28]	62.96		59.49		50.74	
TSM [19]	68.71		63.32		49.72	
SPDNet [10]	65.91		61.16		55.67	
Tensor-CSPNet [15]	75.11		77.36		73.61	
NEUROPHYSNET ^(20,4)	76.23		78.03		74.20	

which include accuracy metrics from the Training Session (T) and Evaluation Session (E).

Filter Bank Common Spatial Pattern (FBCSP) [2], a classical CSP-based method, achieves CV accuracies of 71.29% (T) and 73.39% (E), and a Holdout accuracy of 66.13%. While its ability to extract task-relevant spatial and frequency features is notable, its performance is surpassed by most modern methods due to its inability to model complex temporal and physiological dynamics.

For deep learning-based approaches, ConvNet [20] achieves CV accuracies of 70.42% (T) and 65.89% (E), and a Holdout accuracy of 57.61%. EEGNet [18] performs slightly worse, with CV accuracies of 69.26% (T) and 66.93% (E), and a Holdout accuracy of 60.31%. FBCNet [23], leveraging filter banks to extract multi-band features, achieves CV accuracies of 75.48% (T) and 77.16% (E), and a Holdout accuracy of 71.53%. Despite its superior frequency representation, it does not incorporate physiological dynamics, which constrains its generalization capabilities.

Among Riemannian geometry-based methods, Minimum Distance to Mean (MDM) [28] achieves CV accuracies of 62.96% (T) and 59.49% (E), with a Holdout accuracy of 50.74%. Similarly, Temporal Spectral Mapping (TSM) [21] records CV accuracies of 68.71% (T) and 63.32% (E), and a Holdout accuracy of 49.72%. SPDNet [10] shows slightly better performance than MDM, with CV accuracies of 65.91% (T) and 61.16% (E), and a Holdout accuracy of 55.67%. However, these methods struggle to handle the high-dimensional temporal dynamics inherent in EEG signals, resulting in comparatively low accuracy across all scenarios.

Tensor-CSPNet [15], which extends CSP with tensor-based feature representations, achieves CV accuracies of 75.11% (T) and 77.36% (E), and a Holdout accuracy of 73.61%. This method demonstrates competitive performance by effectively capturing spatial and frequency characteristics. However, it lacks the

integration of physiological insights, limiting its ability to model the temporal dynamics of EEG signals comprehensively.

NeuroPhysNet, on the other hand, achieves the highest performance among all methods in multiple scenarios. It records CV accuracies of 76.23% (T) and 78.03% (E), and a Holdout accuracy of 74.20%. This improvement can be attributed to its innovative integration of the FHN equations. By incorporating the computed membrane potential (v) and recovery variable (w) into Tensor-CSPNet’s feature space, NeuroPhysNet enhances its ability to capture both temporal and physiological dynamics. This fusion allows it to outperform traditional CSP-based methods, Riemannian geometry-based models, and deep learning architectures, while maintaining consistent and robust generalization across diverse evaluation scenarios.

5.2 Impact of Training Data Proportion on NeuroPhysNet Performance

6 Evaluating the Robustness of NeuroPhysNet with Full and Limited Training Data

As a model based on PINNs, NeuroPhysNet inherits one of the prominent advantages of PINNs: the ability to perform well even with limited training data. This capability arises from PINNs’ integration of known physical laws, such as the FitzHugh-Nagumo equations, into the learning process of neural networks. By incorporating physical constraints, NeuroPhysNet reduces its reliance on large-scale datasets and extracts meaningful features even in data-limited scenarios, enhancing its generalization capability.

To evaluate the robustness and performance of NeuroPhysNet under varying training data proportions, we conducted experiments on the BCIC-IV-2a dataset. These experiments compared NeuroPhysNet and Tensor-CSPNet using the full training dataset (100%) and subsets comprising 80%, 50%, and 30% of the training data.

Table 2: Performance Comparison of NeuroPhysNet and Tensor-CSPNet on BCIC-IV-2a Dataset with Varying Training Data Proportions

Data Proportion	Model	CV Accuracy (T)	CV Accuracy (E)	Holdout Accuracy
100%	NEUROPHYSNET	75.85%	76.23%	74.20%
	Tensor-CSPNet	75.11%	77.36%	73.61%
80%	NEUROPHYSNET	74.12%	74.89%	72.15%
	Tensor-CSPNet	73.45%	75.64%	71.32%
50%	NEUROPHYSNET	65.23%	66.72%	64.81%
	Tensor-CSPNet	62.45%	64.31%	59.72%
30%	NEUROPHYSNET	59.41%	60.89%	58.45%
	Tensor-CSPNet	56.12%	58.43%	53.01%

The results in Table 2 reveal a significant performance advantage for NeuroPhysNet over Tensor-CSPNet across all training data proportions, particularly when the data is limited. When using the full training dataset, NeuroPhysNet achieves a CV accuracy of 76.23% (E) and 75.85% (T) and a Holdout accuracy of 74.20%, slightly outperforming Tensor-CSPNet’s 77.36% (E), 75.11% (T), and 73.61% (Holdout). As the training data proportion decreases, the gap between the two models widens considerably.

At 50% training data, NeuroPhysNet achieves a CV accuracy of 66.72% (E) and 65.23% (T) and a Holdout accuracy of 64.81%, while Tensor-CSPNet falls to 64.31% (E), 62.45% (T), and 59.72% (Holdout). This substantial drop in Tensor-CSPNet’s performance demonstrates its higher sensitivity to data scarcity. In contrast, NeuroPhysNet’s integration of FHN equations helps it maintain better generalization by leveraging the physical constraints encoded within its architecture.

At 30% training data, the differences become even more pronounced. NeuroPhysNet achieves a CV accuracy of 60.89% (E), 59.41% (T), and a Holdout accuracy of 58.45%, outperforming Tensor-CSPNet’s 58.43% (E), 56.12% (T), and 53.01% (Holdout) by significant margins. Furthermore, Tensor-CSPNet exhibits less stable predictions across different subjects, which reflects its higher variability compared to NeuroPhysNet.

These results highlight NeuroPhysNet’s superior ability to generalize and remain robust under limited data conditions. By incorporating physiological insights through the FHN equations, NeuroPhysNet captures essential temporal and physiological dynamics, allowing it to outperform Tensor-CSPNet, which primarily relies on tensor-based spatial and frequency representations without physiological integration.

6.1 Evaluating the Impact of v and w Features in NeuroPhysNet

To assess the individual contribution of the physiological features computed by the FHN equations, an experiment was conducted by training and testing NeuroPhysNet using only the membrane potential (v) and recovery variable (w) as input features. This experiment isolates the physiological components from other traditional EEG features to evaluate their standalone effectiveness in EEG classification tasks.

Table 3: Performance of NeuroPhysNet Using Only v and w Features on BCIC-IV-2a Dataset

Data Proportion	CV Accuracy (T)	CV Accuracy (E)	Holdout Accuracy
100%	60.34%	61.23%	59.87%
80%	58.12%	58.94%	57.43%
50%	54.98%	54.32%	52.89%
30%	50.11%	50.89%	49.12%

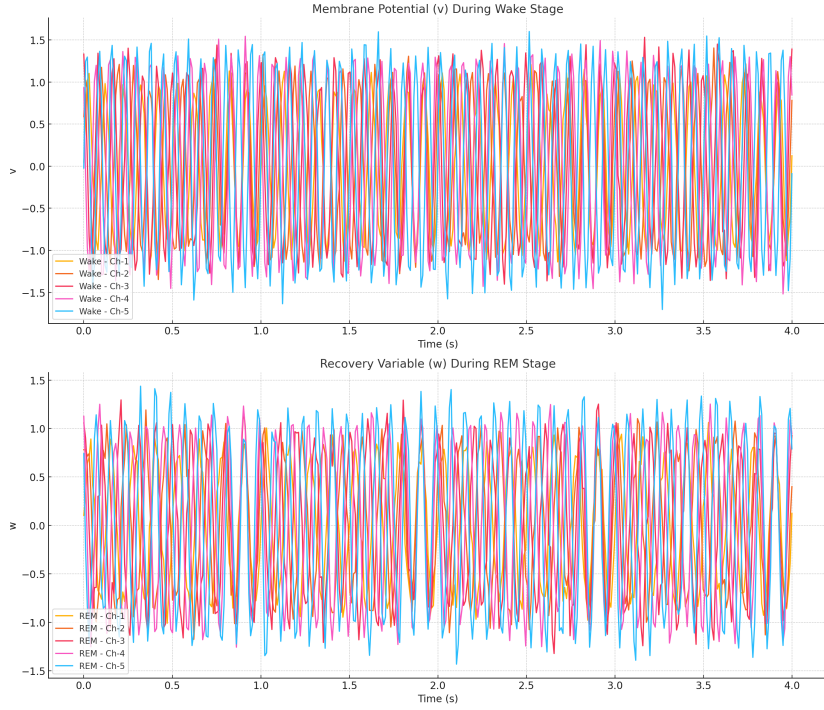


Fig. 1: Visualization of v (membrane potential) during the Wake stage and w (recovery variable) during the REM stage for selected EEG channels. The temporal dynamics of v and w across different channels highlight their variability and potential as features for EEG classification.

The results presented in Table 3 show that using only v and w features, NeuroPhysNet achieves reasonable classification performance, though it is significantly lower than the full-feature model. With the full training dataset, the model achieves a CV accuracy of 61.23% (E) and a Holdout accuracy of 59.87%. As the training data proportion decreases, performance declines but remains relatively stable. For example, at 30% training data, the CV accuracy is 50.89% (E) and 50.11% (T), and the Holdout accuracy is 49.12%. The results indicate that v and w features, derived from the FitzHugh-Nagumo equations, provide valuable discriminative information for EEG classification. Despite the reduced accuracy compared to the full-feature model, the performance remains relatively consistent across different data proportions. This stability demonstrates the robustness of PINNs, particularly in scenarios with limited training data. Moreover, the results emphasize the need to integrate physiological features with traditional EEG features. The full-feature NeuroPhysNet achieves significantly better accuracy by leveraging the complementary strengths of multiple feature types. Future work

could explore more efficient methods for fusing these features to further enhance the model's performance and robustness.

Figure ?? illustrates the temporal dynamics of v and w features for selected EEG channels during the Wake and REM stages, respectively. The variability in frequency, amplitude, phase, and noise across the channels underscores the diverse nature of these features. Such diversity reflects the underlying physiological complexity captured by the FitzHugh-Nagumo equations, which enhances the capability of NeuroPhysNet to model EEG data effectively.

In conclusion, this experiment validates the value of v and w features while highlighting the advantage of combining them with other EEG features. The findings reaffirm the potential of PINNs in data-limited scenarios and their effectiveness in leveraging physiological insights for EEG classification.

7 Conclusion

In this study, we explored the effectiveness of NeuroPhysNet, a model leveraging the FHN equations within the framework of PINNs, for EEG classification tasks. The incorporation of physiological features, specifically the membrane potential (v) and recovery variable (w), was analyzed to assess their standalone contributions and their role in combination with traditional EEG features.

The results demonstrate that v and w features, derived from the FHN equations, capture critical physiological dynamics that contribute significantly to EEG classification, even when used independently. Although their performance is lower than the full-feature model, the use of v and w remains robust across varying training data proportions, highlighting the stability and reliability of PINNs in data-limited scenarios. Furthermore, the integration of v and w with traditional EEG features significantly improves classification accuracy, underlining the complementary nature of these feature sets.

Comparisons with Tensor-CSPNet reveal that NeuroPhysNet achieves superior accuracy and robustness, particularly when training data is limited. The ability of NeuroPhysNet to generalize effectively stems from its integration of physiological insights, which allows it to model complex temporal and spatial dynamics inherent in EEG signals. Additionally, the visualization of v and w features illustrates their diverse temporal patterns across different sleep stages, reinforcing their value as discriminative features.

Overall, this work highlights the potential of PINNs, such as NeuroPhysNet, in addressing challenges in EEG classification, especially in scenarios with constrained data availability. By leveraging physiological equations and integrating them with conventional methods, NeuroPhysNet sets a benchmark for combining domain knowledge with data-driven learning. Future research could focus on optimizing feature fusion strategies, exploring other physiological models, and extending the applicability of NeuroPhysNet to broader EEG datasets and tasks.

Acknowledgments. The authors gratefully acknowledge the computational resources provided by the University of Technology Sydney. Additionally, AI-assisted technology (ChatGPT-4) was utilized for language editing and grammatical refinement.

Disclosure of Interests. The authors declare no conflicts of interest.

References

1. A, M.R., B, P.P., A, G.E.K.: Physics-informed neural networks: A deep learning framework for solving forward and inverse problems involving nonlinear partial differential equations. *Journal of Computational Physics* **378**, 686–707 (2019)
2. Ang, K.K., Chin, Z.Y., Zhang, H., Guan, C.: Filter bank common spatial pattern (fbcsps) in brain-computer interface. In: 2008 IEEE International Joint Conference on Neural Networks (IEEE World Congress on Computational Intelligence). pp. 2390–2397. IEEE (2008)
3. Bijsterbosch, J., Harrison, S.J., Jbabdi, S., Woolrich, M., Beckmann, C., Smith, S., Duff, E.P.: Challenges and future directions for representations of functional brain organization. *Nature neuroscience* **23**(12), 1484–1495 (2020)
4. Cai, S., Wang, Z., Wang, S., Perdikaris, P., Karniadakis, G.E.: Physics-informed neural networks for heat transfer problems. *Journal of Heat Transfer* **143**(6), 060801 (2021)
5. Dickstein, R., Deutsch, J.E.: Motor imagery in physical therapist practice. *Physical therapy* **87**(7), 942–953 (2007)
6. Dou, B., Zhu, Z., Merkurjev, E., Ke, L., Chen, L., Jiang, J., Zhu, Y., Liu, J., Zhang, B., Wei, G.W.: Machine learning methods for small data challenges in molecular science. *Chemical Reviews* **123**(13), 8736–8780 (2023)
7. Garcia Santa Cruz, B., Husch, A., Hertel, F.: Machine learning models for diagnosis and prognosis of parkinson’s disease using brain imaging: general overview, main challenges, and future directions. *Frontiers in Aging Neuroscience* **15**, 1216163 (2023)
8. Hao, Z., Liu, S., Zhang, Y., Ying, C., Feng, Y., Su, H., Zhu, J.: Physics-informed machine learning: A survey on problems, methods and applications. *arXiv preprint arXiv:2211.08064* (2022)
9. Huang, W., Chang, W., Yan, G., Yang, Z., Luo, H., Pei, H.: Eeg-based motor imagery classification using convolutional neural networks with local reparameterization trick. *Expert Systems with Application* (Jan.), 187 (2022)
10. Huang, Z., Van Gool, L.: A riemannian network for spd matrix learning. In: Proceedings of the AAAI Conference on Artificial Intelligence. vol. 31 (2017)
11. Izhikevich, E.M., FitzHugh, R.: Fitzhugh-nagumo model. *Scholarpedia* **1**(9), 1349 (2006)
12. Jagtap, A.D., Kawaguchi, K., Karniadakis, G.E.: Adaptive activation functions accelerate convergence in deep and physics-informed neural networks. *Journal of Computational Physics* **404**, 109136 (2020)
13. Jia, H., Yu, S., Yin, S., Liu, L., Yi, C., Xue, K., Li, F., Yao, D., Xu, P., Zhang, T.: A model combining multi branch spectral-temporal cnn, efficient channel attention, and lightgbm for mi-bci classification. *IEEE Transactions on Neural Systems and Rehabilitation Engineering* **31**, 1311–1320 (2023)
14. Ju, C., Guan, C.: Graph neural networks on spd manifolds for motor imagery classification: A perspective from the time-frequency analysis. *arXiv preprint arXiv:2211.02641* (2022)
15. Ju, C., Guan, C.: Tensor-cspnet: A novel geometric deep learning framework for motor imagery classification. *IEEE Transactions on Neural Networks and Learning Systems* (2022)

16. Ju, C., Guan, C.: Tensor-cspnet: A novel geometric deep learning framework for motor imagery classification. *IEEE transactions on neural networks and learning systems* **12**, 34 (2023)
17. Lawhern, V.J., Solon, A.J., Waytowich, N.R., Gordon, S.M., Hung, C.P., Lance, B.J.: Eegnet: A compact convolutional network for eeg-based brain-computer interfaces. *Journal of Neural Engineering* **15**(5), 056013.1–056013.17 (2018)
18. Lawhern, V.J., Solon, A.J., Waytowich, N.R., Gordon, S.M., Hung, C.P., Lance, B.J.: Eegnet: a compact convolutional neural network for eeg-based brain-computer interfaces. *Journal of Neural Engineering* **15**(5), 056013 (2018)
19. Lin, J., Gan, C., Han, S.: Temporal shift module for efficient video understanding. *corr abs/1811.08383* (2018) (1811)
20. Liu, Y., Shao, H., Bai, B.: A novel convolutional neural network architecture with a continuous symmetry. *arXiv preprint arXiv:2308.01621* (2023)
21. Lotte, F., Bougrain, L., Cichocki, A., Clerc, M., Congedo, M., Rakotomamonjy, A., Yger, F.: A review of classification algorithms for eeg-based brain-computer interfaces: a 10 year update. *Journal of Neural Engineering* **15**(3), 031005 (2018)
22. Lu, J., Tian, Y., Zhang, Y., Ge, J., Sheng, Q.Z., Zheng, X.: Lgl-bci: A lightweight geometric learning framework for motor imagery-based brain-computer interfaces. *arXiv preprint arXiv:2310.08051* (2023)
23. Mane, R., Chew, E., Chua, K., Ang, K.K., Robinson, N., Vinod, A.P., Lee, S.W., Guan, C.: Fbcnet: A multi-view convolutional neural network for brain-computer interface. *arXiv preprint arXiv:2104.01233* (2021)
24. Mao, Z., Jagtap, A.D., Karniadakis, G.E.: Physics-informed neural networks for high-speed flows. *Computer Methods in Applied Mechanics and Engineering* **360**, 112789 (2020)
25. Schirrmeister, R.T., Gemein, L., Eggensperger, K., Hutter, F., Ball, T.: Deep learning with convolutional neural networks for decoding and visualization of eeg pathology. *Human Brain Mapping* **38**(11), 5391–5420 (2017)
26. Tangermann, M., Müller, K.R., Aertsen, A., Birbaumer, N., Braun, C., Brunner, C., Leeb, R., Mehring, C., Miller, K.J., Mueller-Putz, G., et al.: Review of the bci competition iv. *Frontiers in Neuroscience* p. 55 (2012)
27. Tatum, W.O., Rubboli, G., Kaplan, P.W., Mirsatari, S., Radhakrishnan, K., Gloss, D., Caboclo, L., Drislane, F., Koutroumanidis, M., Schomer, D., et al.: Clinical utility of eeg in diagnosing and monitoring epilepsy in adults. *Clinical Neurophysiology* **129**(5), 1056–1082 (2018)
28. Tevet, G., Raab, S., Gordon, B., Shafir, Y., Cohen-Or, D., Bermano, A.H.: Human motion diffusion model. *arXiv preprint arXiv:2209.14916* (2022)
29. Wang, J., Wang, M.: Review of the emotional feature extraction and classification using eeg signals. *Cognitive robotics* **1**, 29–40 (2021)
30. Wang, S., Perdikaris, P.: Long-time integration of parametric evolution equations with physics-informed deeponets. *Journal of Computational Physics* **475**, 111855 (2023)
31. Wang, S., Wang, H., Perdikaris, P.: Learning the solution operator of parametric partial differential equations with physics-informed deeponets. *Science advances* **7**(40), eabi8605 (2021)
32. Yang, J.Q., Wang, R., Ren, Y., Mao, J.Y., Wang, Z.P., Zhou, Y., Han, S.T.: Neuromorphic engineering: from biological to spike-based hardware nervous systems. *Advanced Materials* **32**(52), 2003610 (2020)
33. Yu, R., Wang, R.: Learning dynamical systems from data: An introduction to physics-guided deep learning. *Proceedings of the National Academy of Sciences* **121**(27), e2311808121 (2024)

34. Zhang, D., Lu, L., Guo, L., Karniadakis, G.E.: Quantifying total uncertainty in physics-informed neural networks for solving forward and inverse stochastic problems. *Journal of Computational Physics* **397**, 108850 (2019)